An essential role for an inositol polyphosphate multikinase, Ipk2, in mouse embryogenesis and second messenger production

Joshua P. Frederick*†, Deidre Mattiske†‡, Jessica A. Wofford*, Louis C. Megosh*, Li Yin Drake*, Shean-Tai Chiou*, Brigid L. M. Hogan‡, and John D. York*§

*Departments of Pharmacology and Cancer Biology and Biochemistry, Howard Hughes Medical Institute, and ‡Department of Cell Biology, Duke University, Medical Center, Durham, NC 27710

Communicated by Philip W. Majerus, Washington University School of Medicine, St. Louis, MO, May 4, 2005 (received for review April 13, 2005)

Phospholipase C and several inositol polyphosphate kinase (IPK) activities generate a branched ensemble of inositol polyphosphate second messengers that regulate cellular signaling pathways in the nucleus and cytoplasm. Here, we report that mice deficient for Ipk2 (also known as inositol polyphosphate multikinase), an inositol trisphosphate and tetrakisphosphate 6/5/3-kinase active at several places in the inositol metabolic pathways, die around embryonic day 9.5 with multiple morphological defects, including abnormal folding of the neural tube. Metabolic analysis of *Ipk2*-deficient cells demonstrates that synthesis of the majority of inositol pentakisphosphate, hexakisphosphate and pyrophosphate species are disrupted, although the presence of 10% residual inositol hexakisphosphate indicates the existence of a minor alternative pathway. Agonist induced inositol tris- and bis-phosphate production and calcium release responses are present in homozygous mutant cells, indicating that the observed mouse phenotypes are a result of failure to produce higher inositol polyphosphates. Our data demonstrate that Ipk2 plays a major role in the synthesis of inositol polyphosphate messengers derived from inositol 1,4,5-trisphosphate and uncovers a role for their production in embryogenesis and normal development.

neural tube | phosphoinositides | phytate | signal transduction | calcium signaling

A majority of cellular stimuli have been reported to activate inositol polyphosphate (IP) signaling pathways through phospholipase C dependent inositol 1,4,5-trisphosphate (IP_3) and diacylglycerol production (1, 2). Despite the widespread requirement of inositol signaling activation, it remains an important area of biology to understand how cells use these pathways to elicit selective and diverse responses. The discovery of numerous "orphan" IPs generated downstream of IP_3 first raised the possibility that stimulation of cells and phospholipase C produces a more complex set of IP messengers than previously envisioned (2–4). Agonist-induced production of unique ensembles of >20 IP messengers could create large numbers of "signaling states" that may account for signaling specificity (5).

Further insights into complex IP pathways come from the discovery and characterization of several IP kinases (IPKs) that function downstream of IP_3, thereby enabling the cell to produce various IPs, such as inositol tetrakisphosphate (IP_4), inositol pentakisphosphate (IP_5), inositol hexakisphosphate (IP_6) and inositol pyrophosphates (PP-IP_4 and PP-IP_5) (2, 3, 6, 7). In several eukaryotic cells, the first steps in the conversion of IP_3 to higher IPs occurs through the action of Ipk2, also known as Arg82 and IP multikinase. Ipk2 is a promiscuous kinase capable of phosphorylating the D-6, D-3, and/or D-5 positions on a variety of IP_3/IP_4/IP_5 substrates (see Fig. 1). Initially, Ipk2 was identified in budding yeast, where it functions as a dual-specificity kinase to convert IP_3 to I(1,3,4,5,6)P_5 predominantly through an I(1,4,5,6)P_4 intermediate (8–10). Yeast Ipk2 is nuclear and has been shown to play a role in the regulation of gene expression, chromatin remodeling, and transcription factor stability (9, 11–13). In other eukaryotes, RNA interference and overexpression of Ipk2 have demonstrated that Ipk2 plays a role in the synthesis of IP_5 and IP_6 (14–19). However, the biological function for metazoan Ipk2 has not been identified at this time. Of interest, Ipk2's localization to the nucleus is maintained throughout evolution, consistent with a role in regulating nuclear function.

In this report, we have used homologous recombination to target *Ipk2* for deletion in mice. Cells deficient for Ipk2 appear competent to produce agonist-induced supplies of IP_3 but fail to produce appropriate amounts of higher IPs and to complete the early stages of embryogenesis. Our studies establish a role for Ipk2 in the synthesis of higher IPs in mammals and demonstrate a requirement for the inositol second messenger products of Ipk2 in normal mouse development.

Methods

Reagents. The chemicals used in this study are reagent grade or better. Molecular biology reagents used for PCR, subcloning, Southern analysis, and *in situ* hybridizations were purchased from Takara Mirus Bio (Madison, WI), Sigma, Roche Applied Science, New England Biolabs, or where indicated. Tissue culture medium was obtained from Specialty Media (Phillipsburg, NJ), Sigma, Invitrogen, or the Duke University Cell Culture Facility. [^{3}H]inositol was purchased from American Radiolabeled Chemicals (St. Louis). Oligonucleotide synthesis and DNA sequencing were performed at Integrated DNA Technologies (Coralville, IA) and Duke University, respectively.

Generation and Genotyping of Null Mice. A targeting vector for homologous recombination was constructed by PCR-amplifying R1 ES cell genomic DNA template with Takara Bio Ex Taq polymerase and specific primers. A 4,943-bp PCR fragment containing exon 5 and abutting regions of introns 4 and 5 was cloned into NotI and XhoI sites of the pPNT vector. A 1,184-bp intron 3 PCR fragment was then inserted between PGK-Neo and HSV-TK of the targeting construct at the EcoRI and BamHI sites. The final construct pPNT-IPK2 was linearized with NotI and used for transfection of murine 129/SvEv ES cells. The subsequent homologous recombination leads to the deletion of exon 4, including the region encoding DVKIG, and abutting regions of introns 3 and 4 (diagrammed in Fig. 2*A*).

ES cell transfections, blastocyst injections, and chimeric ani-

Abbreviations: IP, inositol polyphosphate; IP_3, inositol 1,4,5-trisphosphate; IP_4, inositol tetrakisphosphate; IP_5, inositol pentakisphosphate; IP_6, inositol hexakisphosphate; IPK, IP kinase; E*n*, embryonic day *n*; BK, bradykinin.

†J.P.F. and D.M. contributed equally to this work.

§To whom correspondence should be addressed at: Department of Pharmacology and Cancer Biology, Howard Hughes Medical Institute, Duke University Medical Center, DUMC 3813, Durham, NC 27710. E-mail: yorkj@duke.edu.

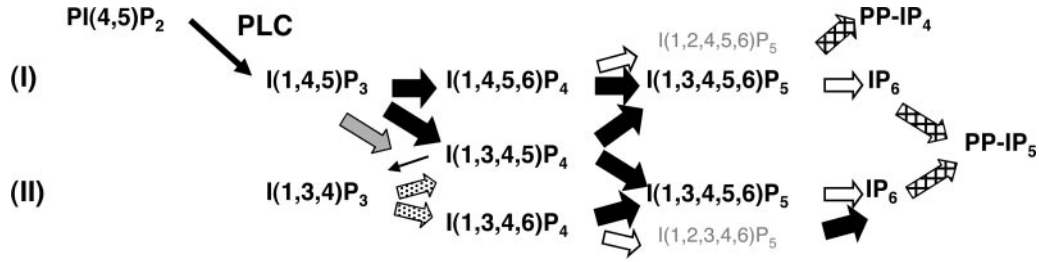

Fig. 1. Complex inositol signaling pathways in mice. Two proposed pathways for IP synthesis in mammals require the activation of phospholipase C (PLC) and conversion of phosphatidylinositol 4,5-bisphosphate, $PI(4,5)P_2$, to $I(1,4,5)P_3$. Pathway I has been shown to exist in *Saccharomyces cerevisiae*, *Arabidopsis, Drosophila melanogaster*, and *Rattus norvegicus* in which $I(1,4,5)P_3$ is converted by Ipk2 (wide black arrows) in two steps to $I(1,3,4,5,6)P_5$ by means of $I(1,4,5,6)P_4$ or $I(1,3,4,5)P_4$ intermediates. Ipk2 also participates in several other reactions as shown. The 2-kinase activity of Ipk1 (wide white arrows) converts IP_5 to IP_6 and is capable of generating branches of $I(1,2,4,5,6)P_5$ or $I(1,2,3,4,6)P_5$. An inositol pyrophosphate synthase (crosshatched arrow) is able to generate inositol pyrophosphate $PP\text{-}IP_4$ or $PP\text{-}IP_5$ species. Pathway II is initiated by an IP_3 3-kinase (gray arrow) that generates $I(1,3,4,5)P_4$ as its sole product, which is then converted to $I(1,3,4)P_3$ by an IP 5-phosphatase (thin arrow) and $I(1,3,4,6)P_4$ by means of a $I(1,3,4)P_3$ 5/6 kinase (stippled arrows). Ipk2 then acts as a 5-kinase to convert $I(1,3,4,6)P_4$ to IP_5, which is a substrate for Ipk1. In both pathways, Ipk2 and Ipk1 function in sequential steps.

mal production was performed at the University of North Carolina (Chapel Hill) Animal Models Core. G418-resistant clones were isolated and screened by PCR. Southern blot analysis was also performed to confirm the recombination of the locus. Two successfully targeted heterozygous ES lines were identified.

One ES clone was used to produce two male chimeric animals by microinjection into C57BL/6 mouse blastocysts. Two founder lines were established by mating the chimeras with female C57BL/6 (The Jackson Laboratories) to generate F1 offspring. These offspring were genotyped by multiplex PCR amplification of genomic DNA by using a single sense primer, F1, located 303 bp upstream of the targeted region and two antisense primers, R1 and R2, located in exon 4 and the Neo cassette, respectively (Fig. 2*A*). PCR conditions were 94°C for 1 min, followed by 30 cycles of denaturation at 98°C for 20 s, annealing and extending at 68°C for 3 min, and a final incubation at 72°C for 7 min. Reaction products were analyzed by electrophoresis through 1% agarose gels. Genomic DNA isolated from ES cells (data not shown) or mouse tissue (Fig. 2*D*) from the wild-type and mutant *Ipk2* loci amplified 2,953-bp and 2,010-bp fragments, respectively.

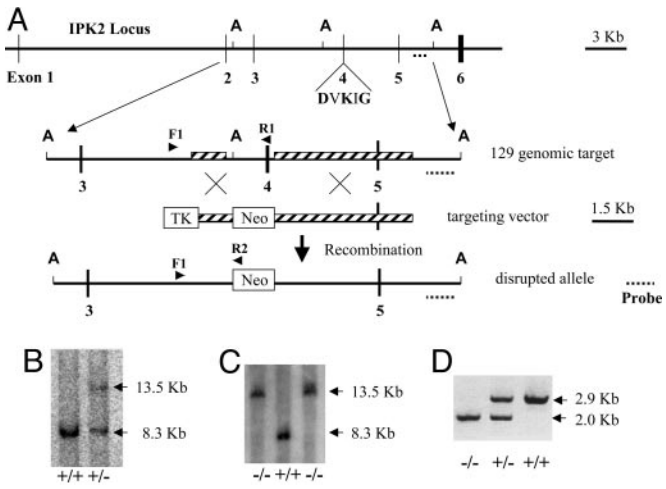

Fig. 2. *Ipk2* gene targeting. (*A*) Targeted disruption of the *Ipk2* locus. Illustration includes part of the *Ipk2* locus, the 129/SvEv genomic target, the targeting vector, and the resulting disrupted *Ipk2* allele. Note the indicated exons (numbered vertical lines), the AvrII (A) restriction sites for Southern analysis, the critical kinase motif DVKIG in exon 4, the Southern probe (dotted line), the regions of targeted homology (hatched boxes), the screening PCR primers (arrows) F1, R1, and R2, and the thymidine kinase and Neo cassettes (open boxes). Exon 4 and adjoining regions of introns 3 and 4 are replaced with the Neo cassette by homologous recombination. (*B*) Southern blot of AvrII-digested genomic spleen DNA from +/+ and +/− mouse siblings. Predicted fragment sizes are 13.5 and 8.3 kb for the targeted and wild-type alleles, respectively. (*C*) Southern blot of AvrII-digested genomic +/+ and −/− ES cell DNA. (*D*) PCR analysis of genomic DNA purified from the embryonic yolk sacs of mouse littermates. Predicted fragment sizes are 2.9 and 2.0 kb for the wild-type and targeted alleles, respectively.

Southern blot analysis was also performed to confirm the recombination of the locus. Ten micrograms of splenic DNA isolated from wild-type or heterozygous littermates was cut with AvrII, fractionated by agarose gel, transferred, and hybridized with an external 3′ probe; a representative result is shown (Fig. 2*B*). Southern analysis was also performed by using genomic DNA isolated from ES cell lines derived from *Ipk2*-null and wild-type ES cells (Fig. 2*C*).

Hematoxylin/Eosin Sections and Whole-Mount *in Situ* Hybridizations. Wild-type and *Ipk2* homozygous null embryos were isolated, fixed in 4% paraformaldehyde in PBS (Invitrogen) overnight at 4°C and rinsed in PBS. Embryonic day (E)0.5 is noon on the day of the vaginal plug. Yolk sac fragments from each embryo were used for genotyping, embryos were embedded in paraffin, and sections were stained with hematoxylin and eosin.

Whole-mount *in situ* hybridizations were performed as follows. Briefly, wild-type E8.5 and E9.5 embryos were isolated, fixed in 4% paraformaldehyde/PBS, dehydrated, rehydrated, washed, and treated with proteinase K (EM Science), fixed in 4% paraformaldehyde/0.1% glutaraldehyde, washed, and preincubated at 57°C with hybridization solution [50% formamide/1.3× SSC (1× SSC = 0.15 M sodium chloride/0.015 M sodium citrate), pH 5.0/0.5% CHAPS/0.1% Tween 20/50 μg/ml yeast tRNA/100 μg/ml heparin/5 mM EDTA] for 1 h. Antisense and sense digoxigenin (DIG)-labeled riboprobes were generated by T7 RNA polymerase from two oppositely oriented clones of the *Ipk2* ORF in pCR2.1 TOPO using a DIG RNA labeling kit according to the manufacturer's specifications (Roche Applied Science). Individual embryos were hybridized overnight at 57°C with similar amounts of sense or antisense probe, washed at 57°C in sequentially increasing stringency, then blocked, probed with 0.375 unit of anti-DIG-alkaline phosphatase Fab fragments per milliliter of block solution, washed extensively, and developed with nitroblue tetrazolium chloride/5-bromo-4-chloro-3-indolyl phosphate, 4-toluidine salt (Roche Applied Science).

ES Cell Isolation, Culture, and Retroviral-Mediated Gene Complementation. Blastocysts were produced by E3.5 pregnant heterozygote intercross females, from which ES cells were isolated and

BIOCHEMISTRY

cultured in the absence of feeder cells according to protocols used by the University of North Carolina Animal Models Core. Three of 11 blastocysts produced individual ES cell lines (lines 2 and 5 were −/− and line 10 was +/+).

Complemented stable cell lines derived from mutant ES lines expressing Ipk2 were generated. The coding sequence was PCR-amplified from cDNA, sequenced, and directionally subcloned into EcoR1/SalI-treated pBabe-Hygro (20). The resulting constructs, pBabe-Ipk2-Hygro and pBabe-Hygro vector control, were then used to generate replication-deficient retroviruses by calcium-phosphate-mediated transfection of the ecotropic phoenix packaging line as described in ref. 21. After double infection, cells were passed in normal ES culture media, and selection was initiated 24 h later by the addition of ES culture medium containing 125 mg/ml hygromycin B (Invitrogen). Hygromycin-resistant ES lines were cultured for 2 weeks and used for labeling studies.

Inositol Radiolabeling of E8.5 Embryos and Derived ES Cells. Embryos from heterozygous crosses were harvested on E8.5 and transferred to a gelatin-coated 48-well tissue culture plate in 200 μl of low inositol medium supplemented with 0.5 mCi/ml (1 Ci = 37 GBq) [^{3}H]myo-inositol. After partial disruption by repeated pipetting, embryonic tissue was incubated for 3 days at 37°C. Tissue fragments were washed extensively and lysed by addition of 0.5 ml of 1 M HCl. After centrifugation, the supernatant containing soluble IPs was removed and snap-frozen. Labeled inositol lipids were extracted from the remaining pellet fraction by using HCl/chloroform/methanol as described in ref. 14. HPLC and TLC analysis were used to separate soluble IPs and phosphoinositides as described in refs. 14 and 22.

The ES cells lines were labeled with [^{3}H]inositol (100 μCi/ml) to assess the soluble IP profiles of cells actively growing in the presence of serum. Filtered lysates were separated by HPLC and eluted at a flow rate of 1.0 ml/min from a Partisphere SAX column (4.6 × 125 mm; Whatman) using a linear gradient of 10 mM to 94.5 mM ammonium phosphate, pH 3.5, over 5 min; 94.5 mM to 517 mM AP over 50 min; 517 mM to 1.7 M AP over 10 min; and constant 1.7 M AP for 34 min.

Agonist-Induced Inositol Metabolism and Calcium Responses. ES cells stimulated with various phospholipase C activators were labeled as described with the following exceptions. Cells were pretreated for 30 min with 20 mM LiCl, incubated for 15 additional min with vehicle, 5 μM bradykinin (BK; Sigma), 100 μM ATP (Sigma), or 5 μM BK/100 μM ATP/20 ng/ml platelet-derived growth factor BB (Upstate Biotechnology, Lake Placid, NY), washed, and lysed in 0.5 M HCl. Soluble radiolabeled extracts were prepared, separated by HPLC, and quantified.

Wild-type and *Ipk2*-null ES cells were incubated in the presence of the ratiometric calcium indicator fura-2 and intracellular calcium levels assessed predominantly as described in refs. 23 and 24. Briefly, cells of both genotype were seeded onto sterile, 0.1% gelatin-coated glass slides, allowed to adhere overnight, and washed with culture medium without phenol red pH indicator. Cells were incubated for 1 h at 37°C in medium containing 4 μM acetoxymethyl ester fura-2 (FluoroPure, Molecular Probes), washed, and perfused. Cells were then sequentially stimulated for ≈100 s with 5 μM BK, washed, treated with 100 μM ATP, washed, and treated a second time with 5 μM BK. The ratio of fluorescence at the emission wavelength of 510 nm of cells alternatively excited at 340 and 380 nm was continuously monitored with a RatioMaster Spectrofluorometer (PTI, South Brunswick, NJ).

Results

Generation of Ipk2 Recombinant ES Cell Lines and Mutant Mice. Identification of the murine *Ipk2* locus on chromosome 10 was performed by using a TBLASTN search of the completed mouse genome with the *Ipk2* coding sequence, similar to what is now referred to as GenBank clone XM 125641. The locus contains six exons and five introns that span ≈34 kb of genomic sequence whose transcription and splicing generates a messenger RNA encoding a 397-aa Ipk2 protein. To disrupt the functionality of Ipk2, we constructed a gene replacement targeting vector that removed exon 4, which encodes residues critical to protein folding and activity (Fig. 2*A*) (9). Recombinant ES cells harboring a wild-type and mutant *Ipk2* allele were identified first by PCR and then confirmed with Southern blot analysis. Two chimeric founders were identified and bred to establish heterozygous F1 offspring.

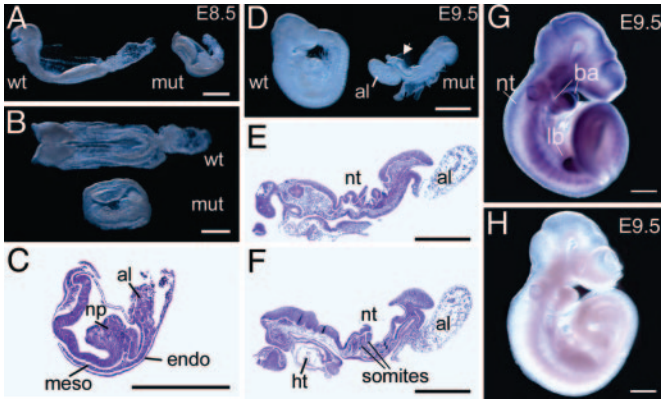

Fig. 3. Morphological analysis of mutant embryos and *in situ* expression of *Ipk2* gene product. Anterior is to the left for all embryos except mutant in *D*. (*A* and *B*) Embryos collected on E8.5 viewed laterally (*A*) and dorsally (*B*). Note smaller size of the mutant embryo (mut) compared with wild type (wt). (*C*) Section through a mutant embryo with similar morphology to that shown in *A* and *B*. Note the folded neural plate (np) and small allantois (al). Mesodermal (meso) and endodermal (endo) layers are also marked. (*D*) Embryos on E9.5 viewed laterally. The wild-type embryo has turned but not the mutant embryo, which has a small, abnormal allantois and folded neural tube (nt; arrow). (*E* and *F*) Two sections from a series through a mutant embryo. Note the folded neural tube, somites, fore and hind gut, and heart trabeculae (ht). (*G* and *H*) *In situ* whole-mount expression analysis of E9.5 wild-type embryos hybridized with antisense (*G*) or sense (*H*) negative control RNA. Note the high level of expression of *Ipk2* transcript (purple staining) in the neural tube, branchial arches (ba), hind limb bud (lb), somites, and head region. No specific staining above background is observed in *H*. (Scale bars, 500 μm.)

Loss of *Ipk2* Exon 4 Results in Early Embryonic Lethality. Heterozygous mice derived from the F1 animals were overtly normal and fertile and have been maintained as a breeding colony for >1.5 years. During this time, we have analyzed F2 progeny from >20 heterozygous matings, including >200 pups, and have not identified any living or stillborn homozygous *Ipk2*-null pups. Wild-type and heterozygous pups were born in normal numbers at a 1:2 ratio consistent with the hypothesis that loss of both alleles of *Ipk2* is embryonic lethal.

To determine the timing of the embryonic lethality, we examined embryos at different stages, focusing on early to mid gestation periods. From E10.5 through E12.5 approximately one in four embryos appeared to be inviable and in the process of reabsorption. By E9.5, all embryos appeared viable, although ≈20% were smaller than their littermates. Microdissection and genotyping of these embryos confirmed they were *Ipk2*-null.

Morphological Phenotype of Homozygous Null Embryos. By E8.5, homozygous null embryos dissected from the yolk sac and amnion were clearly smaller and shorter along the anterior–posterior axis than wild-type littermates and were developmentally delayed (Fig. 3 *A* and *B*). An allantois was present but did not appear to fuse with the chorion. Viewed dorsally, no somites

were visible, compared with the six to eight somites present in wild type, and there was abnormal folding of the neural tube. Analysis of serial sections (Fig. 3*C*) showed that extraembryonic tissues (chorion, yolk sac endoderm and mesoderm with blood islands, and amnion) were relatively normal. The embryo was underlain by a layer of definitive endoderm. Mesoderm was present in the midline and under the anterior neural folds, but there was no evidence that somites had formed. The most striking abnormality was the massive accumulation and folding of neurectoderm in the mid-hind region of the embryo.

By E9.5, control embryos but not homozygous mutants had turned. In the mutants, the allantois had still not fused with the chorion, and the anterior neural tube was open (Fig. 3*D*). Serial sectioning showed that approximately six somites had formed, and fore and hind gut pockets were clearly present (Fig. 3 *E* and *F*). The heart was localized ventrally and had both myocardial and endocardial layers. Again, the most obvious defect was the prominent folding and kinking of the neural tube.

Expression Pattern of *Ipk2*. To assess the expression during this critical period of development, whole-mount *in situ* hybridization was performed on wild-type embryos harvested around E8.5 (data not shown) and E9.5 (Fig. 3 *G* and *H*). By E8.5, expression of *Ipk2* was mainly in the head folds and along the length of the neural tube, whereas no expression was detected in the developing heart. By E9.5, the antisense probe showed the highest expression in the head and branchial arches, along with persistent expression in the neural tube (Fig. 3*G*). Staining was also present in developing somites and in the developing hind limb bud (Fig. 3*G*). Minimal staining was observed with the sense probe (Fig. 3*H*).

Inositol Labeling of Mutant Embryos and Derived ES Cells. To assess the role for Ipk2 in the production of higher IPs, we performed metabolic radiolabeling of +/+, +/−, and −/− embryos harvested on E8.5. Mechanically disrupted embryo fragments were radiolabeled with inositol precursor, and soluble IPs and phoshophoinositides (inositol lipids) were analyzed. HPLC separation of soluble IPs (Fig. 4*A*) showed poor but consistent labeling efficiency as judged by a small peak of IP_6 relative to the similarly large peak of inositol in all extracts. Samples harvested from the −/− embryos showed no detectable IP_6 peak in >10 analyzed samples. By contrast, the heterozygous and wild-type samples showed similar profiles for IP_6. We also analyzed the levels of phosphatidylinositol, phosphatidylinositol phosphate, and phosphatidylinositol 4,5-bisphosphate by TLC and found them to be indistinguishable among all three genotypes, indicating that the labeling efficiency and lipid metabolic pathways of each genotype were normal (data not shown).

Isolation and Characterization of Homozygous Mutant ES cells. To further characterize the role of Ipk2 at the cellular level, we attempted to culture cells from E8.5 and E9.5 embryos without success. We then isolated ES cells from E3.5 blastocysts under feeder-free conditions. Three independent ES lines (lines 2 and 5 were −/− and line 10 was +/+) were isolated and have been maintained in culture for >25 passages in the absence of feeder cells.

To assess the effects of *Ipk2* loss on IP metabolism, the wild-type and mutant ES lines were radiolabeled with [3H]inositol precursor over several doublings. The efficiency of labeling of all three ES lines was excellent, and multiple IPs ranging from IP_1 were easily detectable (Fig. 4*B*). Analysis of the IP profiles from wild-type and null ES lines (only lines 10 and 2 are shown) showed an ablation of $I(1,3,4,5,6)P_5$ and IP_2x, and a >90% reduction of IP_6 in the −/− cells. The inositol pyrophosphate PP-IP_5 (also known as IP_7) was detected at low levels in wild-type cells but was not observed in mutant lines (data not shown). The levels of $I(1,4)P_2$, $I(3,4)P_2$, $I(1,3,4)P_3$, $I(1,4,5)P_3$, and IP_4 were slightly decreased or similar in mutant cells as compared with normal counterparts. Abundant endogenous IP phosphatase activities likely account for the failure to observe Ipk2 substrate accumulation in these mutant cells. The identity of each isomer was confirmed by coelution with known standards and/or sensitivity to conversion by several recombinant inositol kinases and phosphatases. Of interest, the IP_4 peak does not appear to be either $I(1,3,4,5)P_4$ or $I(1,4,5,6)P_4$, and further characterization is required for identification. Quantification of levels of each species of IP was determined through radiolabeling of each cell line in multiple experiments (Fig. 5*A left*).

To confirm that alterations in the IP profiles observed in the homozygous null lines were a direct result of loss of Ipk2, we rescued ES lines with retrovirally delivered *Ipk2*. Lines 2 and 5 (both −/−) were infected with control (empty) and Ipk2-expressing retroviruses and selected for hygromycin resistance,

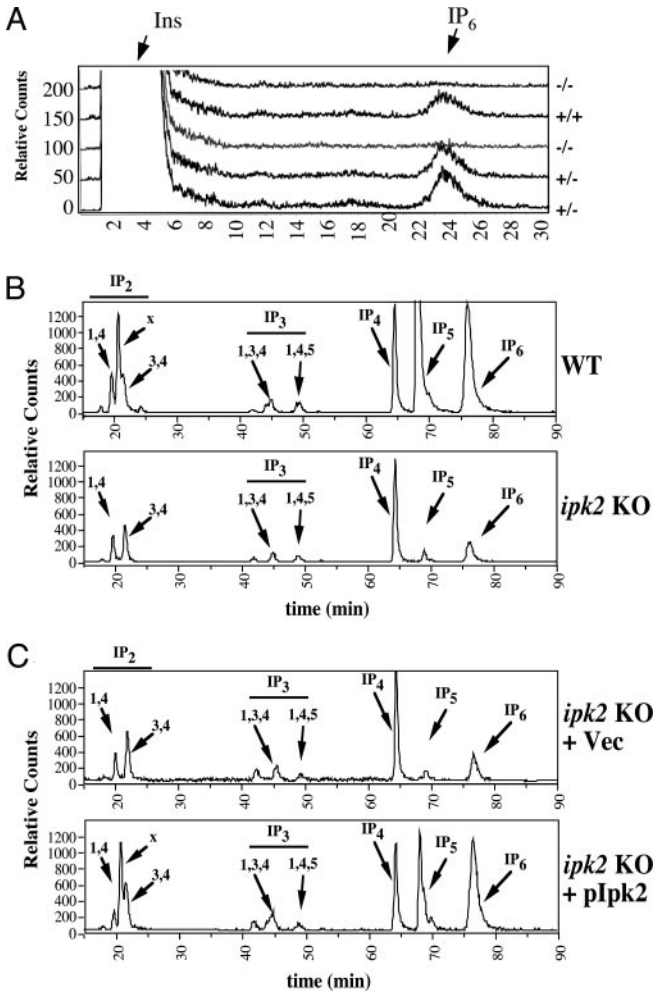

Fig. 4. Analysis of inositol metabolism in *Ipk2* mutant embryos and ES cells. (*A*) Embryos were harvested on E8.5 and labeled with [^{3}H]inositol as described in *Methods*. Radiolabeled IPs were extracted and separated by strong-anion HPLC as shown. Representative chromatograms are shown for each genotype noting the absence of IP_6 production in −/− embryos. (*B*) ES cells were derived from E3.5 blastocysts and radiolabeled with [^{3}H]inositol for several doublings. Soluble IPs from wild-type (*Upper*) and null (*Lower*) lines were separated by HPLC. The elution position of IP standards are marked by arrows. (*C*) Analysis of IPs derived from radiolabeled extracts obtained from complemented ES line 5 (−/−) with vector control (*Upper*) or Ipk2-expressing retrovirus (*Lower*). Similar results were observed in complemented ES line 2 (data not shown). Note the restoration of IP_2x, IP_5, and IP_6 synthesis upon expression of Ipk2, confirming its direct or indirect role in their production.

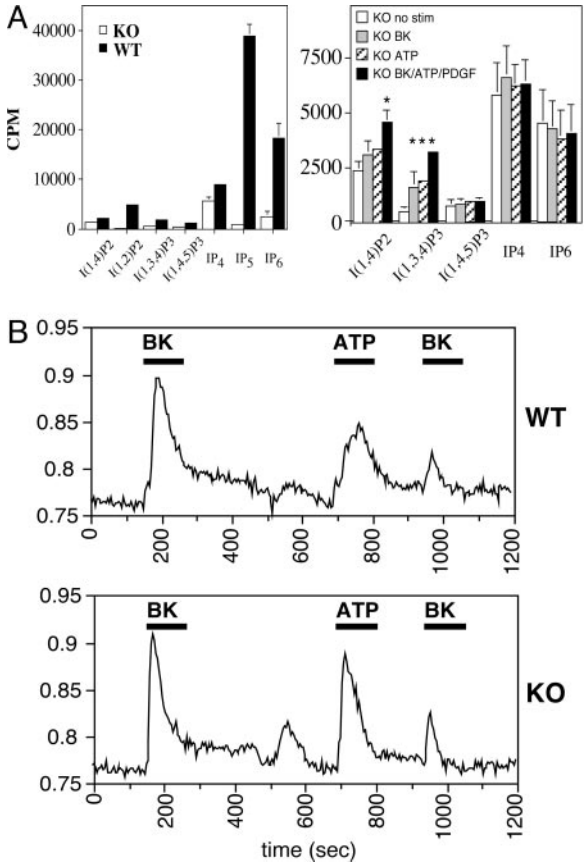

Fig. 5. Agonist-induced inositol metabolism and calcium responses in ES cell lines. (*A*) (*Left*) Quantification of various IP species isolated from radiolabeled extracts of serum-replete wild-type control or *Ipk2* mutant ES cells. Knockout (KO) (−/−) data are a compilation of lines 2 and 5, and error bars are shown. (*Right*) Analysis of IP metabolites in agonist-induced knockout lines 2 and 5. Cells were stimulated for 15 min with vehicle control, 5 μM BK, 100 μM ATP, or BK/ATP/platelet-derived-growth factor. Lithium is added to cells before extraction to inhibit IP phosphatases, thereby enabling visualization of agonist-induced IP_2 and $I(1,3,4)P_3$ peaks. It is presumed that these messengers are derived from $I(1,4,5)P_3$ production and breakdown. Asterisks indicate a two-tailed *t* test ($P < 0.02$). (*B*) Agonist-induced calcium signaling responses in wild-type (*Upper*) and *Ipk2*-null (*Lower*) ES lines. Ratiometric imaging of fura-2 dye provides a measure of the relative increase of intracellular calcium in response to sequential 5 μM BK, 100 μM ATP, and then 5 μM BK treatments. Black bars represent the duration of stimulus for each agonist.

indicating the stable integration of the viral DNA. Complemented −/− mutant ES cells were again radiolabeled over several doublings, and the IP profiles were assessed (Fig. 4*C*). IP profiles from ES line 5 expressing Ipk2 showed nearly complete complementation of IP_6 and IP_2x production and partial restoration of IP_5 synthesis as compared with vector control ES line 5 (Fig. 4*C Lower*) and wild-type ES line 10 (Fig. 4*B Upper*).

Agonist-Induced IP and Calcium Responses in Mutant and Wild-Type ES Cells. To determine whether agonist-induced activation of phospholipase C and metabolism of $I(1,4,5)P_3$ were functioning in the absence of Ipk2, we analyzed IPs from mutant ES cells treated with BK, ATP, or with BK/ATP/platelet-derived-growth factor. Given the transient nature of IPs, we pretreated cells with lithium to inhibit inositol phosphatases and found that stimulation resulted in increases in $I(1,4)P_2$ and $I(1,3,4)P_3$ levels (Fig. 5*A Right*). These species serve as indicators that stimulation resulted in increased IP_3 production and breakdown.

We also used a ratiometric method for measuring intracellular calcium release in our mutant and wild-type lines in response to agonist. Cells were first treated with 5 μM BK, and wild-type and knockout lines showed similar agonist-induced intracellular calcium responses (Fig. 5*B*). After washing out the agonist and allowing the cells a short recovery period, we added 100 μM ATP to the same cells and found again a significant rise and fall in intracellular calcium levels in both lines (Fig. 5*B*). Agonist-induced desensitization was analyzed by repeating the BK stimulus after the initial regime, and we observed a similar decrease in calcium release in wild-type and mutant cells. Importantly, the peak shapes defined by inspection of leading and trailing edges and ratio of peak height to duration were comparable in both lines and for each agonist, generally indicating that the loss of Ipk2 did not significantly alter the latency of IP_3-mediated calcium signaling.

Discussion

It is highly significant that *Ipk2*, a gene that encodes a kinase whose function includes the conversion of IP_3 and IP_4 to higher phosphorylated IPs, is required for proper development of the mammalian embryo. This finding provides strong evidence that the orphan IP products generated by the enzyme or downstream metabolites play a critical role in mammalian cells. These conclusions are also nicely supported by the work of Verbsky *et al*. (25) presented in this issue of PNAS, which describes an essential role for mouse *Ipk1* in embryogenesis. Ipk2 and Ipk1 function sequentially in the production of IP_6 (see Fig. 1). The similar lethal phenotypes, inositol metabolism defects, and localization of the kinases to developing neural tissues in the mouse embryo support the involvement of these messengers, especially IP_5 and/or IP_6, in specific morphogenetic processes. The variations in phenotypes between the two kinase mutants may result from activities that generate unique IP messengers whose production are not linked, for example $I(1,2,3,4,6)P_5$ and $I(1,4,5,6)P_4$, which are independent products of Ipk1 and Ipk2 reactions, respectively (Fig. 1).

Homozygous *Ipk2*-null mutants are smaller than normal and developmentally delayed. Our observations that mutants do not appear to develop beyond E9.5–E10 is consistent with the failure of the allantois to fuse with the chorion, because the formation of this connection is essential for establishing a nutritional connection between the embryo and mother. In addition to the defect in the allantois, the most obvious abnormalities are delayed formation of somites and the characteristic folding and kinking of the neural tube.

The absence of Ipk2 clearly does not prevent the morphogenetic and differentiation processes associated with gastrulation because the homozygous null embryos contain representatives of all three germ layers (ectoderm, endoderm, and mesoderm), nor is it required for viability of ES cells. However, the delayed formation of the somites and the kinking of the neural tube are compatible with abnormalities in the proliferation, differentiation, and/or morphogenesis of embryonic mesoderm or neuroectoderm. Furthermore, the expression pattern of *Ipk2* in E8.5 to E9.5 embryos indicates enrichment in the neural tube, consistent with the defects observed. Extraembryonic mesoderm contributing to the allantois may also be affected. Similar morphological defects have been reported in several mouse mutants. For example, embryos homozygous null for *Fgf receptor1* (*Fgfr1*) have a very similar small size, reduced elongation along the anterior–posterior axis, absence of somites by E8.5, and kinked neural tube (26, 27). Subsequent analysis revealed that nascent mesodermal cells lacking Fgfr1 have defects in the down-regulation of E-cadherin, the activation of downstream targets of Wnt signaling, and the ability to migrate away from the primitive streak (28, 29). The kinking of the neural tube characteristic of *Fgfr1*-null mutants is thought to be secondary to the failure of axial and paraxial mesoderm to migrate along the

anterior-posterior axis underneath the neuroectoderm. Similar abnormalities in mesoderm patterning and morphogenesis have been reported in mouse embryos lacking *Shp2*, which encodes a Src homology 2 domain-containing tyrosine phosphatase modulating the intensity and duration of intracellular signaling from receptor tyrosine kinases, including Fgfr1 (30).

Given Ipk2's role in yeast as a regulator of gene expression, it is tantalizing to speculate that the developmental defects observed relate to specific defects in chromatin remodeling or gene transcription in specific tissues (9, 11–13). The nuclear localization of mammalian Ipk2 is maintained, and loss of Ipk2 in these programs may repress or activate specific developmentally transcribed targets. Alternatively, production of IP products may directly impact the functionality of developmentally important proteins involved in cell behavior, adhesion, and/or migration. It is also possible that, because the products of Ipk2 serve as precursors to a number of other putative IP messengers, the effects observed are indirectly related to loss of these downstream signaling pathways, such as mRNA export (8, 31), DNA end-joining (32), DNA metabolism (33), telomere maintenance (34), and/or membrane trafficking (35, 36). The ability to culture ES cells derived from *Ipk2*-null blastocysts will greatly enhance studies aimed at dissecting the mechanism by which loss of Ipk2 and its IP products results in these striking phenotypes.

We end by noting that Ipk2 is one of the earliest known evolutionarily conserved kinases within the inositol signaling pathway. Ipk2 appears to be the ancestor for IP_3 kinases as well as inositol pyrophosphate synthases (also known as IP_6Ks). Interestingly, it seems that IP_3-mediated calcium release evolved later and is not thought to be present in lower eukaryotes, such as budding yeast. As we began these studies, it was not clear whether the Ipk2 pathways important for regulating nuclear processes in yeast would still be functionally important in higher eukaryotes. Given the proposed roles for calcium signaling in modulating nuclear events, it was certainly plausible that organisms that evolved calcium signaling may have no longer needed to produce higher IPs. Based on the lethality of the *Ipk2*- and *Ipk1*-null mutations in mice, it is now readily clear that these kinases and presumably many of their IP messenger products are critically important in mammals. Collectively, these data support the initial idea, presented in the Introduction, that IP signaling comprises an ensemble of messengers whose patterns are used to determine signaling specificity. For those studying the effects of agonist-induced activation of inositol signaling in mammalian cells, it seems prudent to consider possible roles for IP_5, IP_6, and inositol pyrophosphate messengers.

Note. As this manuscript was being revised, we learned of recent work at the Wente laboratory (Vanderbilt University Medical Center, Nashville, TN) demonstrating that down-regulation of Ipk1 in zebrafish embryos resulted in developmental abnormalities, including left–right asymmetry (37).

We thank past and present members of the J.D.Y. laboratory for helpful discussions; Batsirayi Mutamba for technical assistance; Drs. Barbara Buckley, Zermeena Mirza, and Richard Whorton (Duke University) for assistance with the intracellular calcium measurements; the University of North Carolina (Chapel Hill) Animal Models Core facility, specifically Dr. Randy Thresher, Kimberly Kluckman, and Ray Fox; and the Majerus and Wente laboratories for sharing information. This work is supported by funds from the Howard Hughes Medical Institute (to J.D.Y.) and National Institutes of Health Grant HL-55672 (to J.D.Y).

1. Berridge, M. J. & Irvine, R. F. (1989) *Nature* **341,** 197–205.
2. Majerus, P. W. (1992) *Annu. Rev. Biochem.* **61,** 225–250.
3. Irvine, R. F. & Schell, M. J. (2001) *Nat. Rev. Mol. Cell. Biol.* **2,** 327–338.
4. York, J. D., Guo, S., Odom, A. R., Spiegelberg, B. D. & Stolz, L. E. (2001) *Adv. Enzyme Regul.* **41,** 57–71.
5. York, J. D. & Hunter, T. (2004) *Science* **306,** 2053–2055.
6. York, J. D. (2003) *Handbook of Cell Signaling* (Academic, New York).
7. Shears, S. B. (2004) *Biochem. J.* **377,** 265–280.
8. York, J. D., Odom, A. R., Murphy, R., Ives, E. B. & Wente, S. R. (1999) *Science* **285,** 96–100.
9. Odom, A. R., Stahlberg, A., Wente, S. R. & York, J. D. (2000) *Science* **287,** 2026–2029.
10. Saiardi, A., Caffrey, J. J., Snyder, S. H. & Shears, S. B. (2000) *FEBS Lett.* **468,** 28–32.
11. Shen, X., Xiao, H., Ranallo, R., Wu, W. H. & Wu, C. (2003) *Science* **299,** 112–114.
12. Steger, D. J., Haswell, E. S., Miller, A. L., Wente, S. R. & O'Shea, E. K. (2003) *Science* **299,** 114–116.
13. El Alami, M., Messenguy, F., Scherens, B. & Dubois, E. (2003) *Mol. Microbiol.* **49,** 457–468.
14. Fujii, M. & York, J. D. (2005) *J. Biol. Chem.* **280,** 1156–1164.
15. Nalaskowski, M. M., Deschermeier, C., Fanick, W. & Mayr, G. W. (2002) *Biochem. J.* **366,** 549–556.
16. Saiardi, A., Nagata, E., Luo, H. R., Sawa, A., Luo, X., Snowman, A. M. & Snyder, S. H. (2001) *Proc. Natl. Acad. Sci. USA* **98,** 2306–2311.
17. Seeds, A. M., Sandquist, J. C., Spana, E. P. & York, J. D. (2004) *J. Biol. Chem.* **279,** 47222–47232.
18. Verbsky, J. W., Chang, S. C., Wilson, M. P., Mochizuki, Y. & Majerus, P. W. (2005) *J. Biol. Chem.* **280,** 1911–1920.
19. Stevenson-Paulik, J., Odom, A. R. & York, J. D. (2002) *J. Biol. Chem.* **277,** 42711–42718.
20. Morgenstern, J. P. & Land, H. (1990) *Nucleic Acids Res.* **18,** 3587–3596.
21. Ito, A., Kawaguchi, Y., Lai, C. H., Kovacs, J. J., Higashimoto, Y., Appella, E. & Yao, T. P. (2002) *EMBO J.* **21,** 6236–6245.
22. Guo, S., Stolz, L. E., Lemrow, S. M. & York, J. D. (1999) *J. Biol. Chem.* **274,** 12990–12995.
23. Dolor, R. J., Hurwitz, L. M., Mirza, Z., Strauss, H. C. & Whorton, A. R. (1992) *Am. J. Physiol.* **262,** C171–C181.
24. Buckley, B. J. & Whorton, A. R. (1997) *Am. J. Physiol.* **273,** C1298–C1305.
25. Verbsky, J., Lavine, K. & Majerus, P. W. (2005) *Proc. Natl. Acad. Sci. USA* **102,** 8448–8453.
26. Deng, C. X., Wynshaw-Boris, A., Shen, M. M., Daugherty, C., Ornitz, D. M. & Leder, P. (1994) *Genes Dev.* **8,** 3045–3057.
27. Yamaguchi, T. P., Harpal, K., Henkemeyer, M. & Rossant, J. (1994) *Genes Dev.* **8,** 3032–3044.
28. Ciruna, B. G., Schwartz, L., Harpal, K., Yamaguchi, T. P. & Rossant, J. (1997) *Development (Cambridge, U.K.)* **124,** 2829–2841.
29. Ciruna, B. & Rossant, J. (2001) *Dev. Cell.* **1,** 37–49.
30. Saxton, T. M., Henkemeyer, M., Gasca, S., Shen, R., Rossi, D. J., Shalaby, F., Feng, G. S. & Pawson, T. (1997) *EMBO J.* **16,** 2352–2364.
31. Feng, Y., Wente, S. R. & Majerus, P. W. (2001) *Proc. Natl. Acad. Sci. USA* **98,** 875–879.
32. Hanakahi, L. A., Bartlet-Jones, M., Chappell, C., Pappin, D. & West, S. C. (2000) *Cell* **102,** 721–729.
33. Huang, K. N. & Symington, L. S. (1995) *Genetics* **141,** 1275–1285.
34. York, S. J., Armbruster, B. N., Greenwell, P., Petes, T. D. & York, J. D. (2005) *J. Biol. Chem.* **280,** 4264–4269.
35. Dubois, E., Scherens, B., Vierendeels, F., Ho, M. M., Messenguy, F. & Shears, S. B. (2002) *J. Biol. Chem.* **277,** 23755–23763.
36. Saiardi, A., Caffrey, J. J., Snyder, S. H. & Shears, S. B. (2000) *J. Biol. Chem.* **275,** 24686–24692.
37. Sarmah, B, Latimer, A. J., Appel, B. & Wente, S. R. (2005) *Dev. Cell*, in press.